Microwave-Assisted, Preparation, Characterization, and Biological Activities of Schiff Bases Derived from 4-Aminoantipyrine with Acetonylacetone for Some New Rare-Earth Metals

Kawther Adeeb Hussein[1*], Naser Shaalan[2], and Marwa Faeq[1]

[1]*Department of Chemistry, College of Science, Al-Nahrain University, Jadria, Baghdad 10072, Iraq*

[2]*Department of Chemistry, College of Science for Women, University of Baghdad, Baghdad 10071, Iraq*

* ***Corresponding author:***

tel: +964-7805758871
email: kawther.adeeb@nahrainuniv.edu.iq

Received: April 7, 2024
Accepted: June 16, 2024

DOI: 10.22146/ijc.95419

Abstract: *Five new lanthanide complexes based on azomethine (Schiff bases) ligands have been synthesized, including La, Nd, Er, Gd, and Dy. Complexes were synthesized using the azomethine Schiff bases resulting from condensation reactions between 4-aminoantipyrine and acetonylacetone. The structural characteristics of azomethine obtained are characterized quantitatively and qualitatively through various techniques, including elemental analyses, magnetic susceptibility measurement, molar conductivity, infrared, ultraviolet absorption, GC-mass, and* ^{1}H- *and* ^{13}C-NMR *spectroscopy studies. The structural characteristics of* Ln^{+3} *complexes indicate that the complexes possess a composition of a specific type. Based on the elemental analyses, magnetic susceptibility measurement, molar conductivity, and ultraviolet absorption spectroscopy data, it can be inferred that the central metal ion is surrounded by a coordination number of 10, the general formula of* $[Ln(L)_2(NO_3)]\cdot nNO_3nH_2O$. *The physical measurements confirmed that the synthesized complexes exhibit non-electrolyte behavior and paramagnetic properties. The antibacterial activity of the compounds was assessed* in vitro *against 4 pathogenic strains:* E. coli, S. aureus, K. pneumoniae, *and* S. mutans. *The evaluation was conducted using the agar disc spreading method. The results demonstrated that certain complexes exhibited significant antibacterial efficacy in comparison to the biological activity of the ligand.*

Keywords: *Schiff base; lanthanide; biological activity; microwave; 4-aminoantipyrine*

INTRODUCTION

Microwaves exhibit a wavelength range of 0.1 to 100 cm, corresponding to frequencies ranging of 0.3 to 300 kHz. These waves are situated between the far infrared and radio waves. Microwaves cannot break bonds because the energy is insufficient. Photon is a form of energy, not thermal energy. Their interaction with the medium through which they can be reflected, transmitted, or absorbed transforms them into heat. Rays are converted by some liquids or solids. Heat is produced by electromagnetism, which results in chemical reactions. As a result of the interest in microwave-assisted chemical synthesis, this method grew rapidly. The use of this technology has opened up new opportunities for the chemical synthesis of compounds that cannot be synthesized using conventional heat. Microwave radiation interactions have been extensively researched since its initial application by Gedye and Majetich in 1986. Inorganic and organic compounds are synthesized utilizing this technology, especially cyclic compounds, which have high biological effectiveness [1-3].

In recent decades, there has been significant interest in Lanthanide Schiff base complexes due to their possible applications in magnetism, catalysis, antioxidants, and medicine [4-6]. Among the numerous organic ligands, the Schiff base ligands coordinate with transition metals and lanthanide ions, leading to a diverse family of coordination complexes [7]. It is possible to synthesize Schiff base ligands by reacting aldehydes and ketones with primary

amines under suitable conditions and which contain carbon-nitrogen double bonds (C=N) [8-9]. These ligands could coordinate easily with metals [10-11]. Based on the central atom's reaction conditions and influential factors, metal chelates tend to form at the ligand's multiple donor sites in various coordination modes. These coordination C=N linkage plays a crucial role in the biological activity of azomethine derivatives [12-13]. Particular azomethines have been recorded to demonstrate remarkable antibacterial, antifungal, anticancer, and antimalarial characteristics [14]. Coordination compounds have attracted the interest of scientists due to their diverse range of biological activities and functional properties. In the realm of medicinal chemistry, the development of novel compounds exhibiting enhanced antibacterial and anticancer properties is of the utmost importance [15-16].

In biological systems, 4-aminoantipyrine derivatives are crucial biomodel compounds because of their possible pharmacological, medicinal, and biological applications [17]. The investigation of new bioactive compounds derived from 4-aminoantipyrine is of the utmost importance due to their potential as analgesic, anticancer, antibacterial, and antiviral medications [18-19]. Coordination chemistry frequently employed 4-aminoantipyrine derivatives due to their capacity to form coordination bonds with keto or azomethine groups. Derivatives of Schiff bases and 4-aminoantipyrine exhibit potential as antibacterial agents [20-21]. It presents synthesis methods and exciting structures of complexes containing lanthanide ions $[Ln(NO_3)_3]\cdot 6H_2O$, Ln = La^{+3}, Nd^{+3}, Er^{+3}, Gd^{+3}, and Dy^{+3}, as well as a summary of the role of lanthanides and their compounds in the diagnosis and study of biological efficacy.

■ EXPERIMENTAL SECTION

Materials

Reagents and compounds utilized in the study included were acetonylacetone (96%), 4-aminoantipyrine (97%), absolute ethanol (99%), and lanthanide nitrate $[Ln(NO_3)_3]\cdot 6H_2O$, where Ln^{+3} = La^{+3}, Nd^{+3}, Er^{+3}, Gd^{+3}, and Dy^{+3}. All materials are supplied and used by Sigma Aldrich. In this study, some of the bacteria used were gram-negative bacteria, namely *E. coli* (ATCC-8739) and *K. pneumonia* (ATCC-13883), as well as gram-positive bacteria, namely *S. aureus* (ATCC-25923) and *S. mutans* (ATCC-25175).

Instrumentation

Phi nano science center micro was used to analyze the ligands and complexes under investigation using a Thermos Finnegan flash device. We used a Shimadzu FTIR spectrometer 8400Sranged from 4000 to 250 cm^{-1} to measure the IR spectra of the ligand and their complexes. A KBr disk was used for the ligand, and a CsI disk was used for the complexes. The microanalysis of the ligand and complexes was conducted using a Thermo Finnegan flash device Energy Center in Syria. We conducted magnetic spectroscopy on the ligand that was diagnosed in Tehran, Iran, specifically using ^{1}H- and ^{13}C-NMR techniques. We utilized a Bruker 400 MHz AVANCE spectrometer to examine the ligands, which were dissolved in DMSO-d_6 solvent. We utilized $Si(CH_3)_4$ (TMS) as a reference to measure the spectra. The phi nano science center recorded the GC-mass spectra of the prepared ligand using a network mass-selective device. An English company's Stuart devices were used to determine the melting points of the ligand and its complexes. The remarkable temperature range of this apparatus is 300 °C. The chemistry lab in the College of Science for Women at the University of Baghdad served as the experimental site.

Procedure

Preparation of azomethine ligand (Schiff bases)

Preparing an azomethine Schiff base was conducted by mixing in the crucible a stoichiometric 1.0000 g (1.0 mol) of acetonylacetone with 3.5614 g (2.0 mol) of 4-aminoantipyrine and adding 4 drops of glacial acetic acid. The mixture was put in microwave irradiation at 170 W for 4 min. The yellowish-white precipitate was filtered, collected, and then dried for 24 h before recrystallizing from heated absolute ethanol. After filtering the yellowish-white powder, it was collected and allowed to dry for 10–15 h. The general route of azomethine ligand synthesis is depicted in Scheme 1. The Schiff base ligand was characterized by several techniques [22-23].

Preparation of the lanthanide metal complexes

The lanthanide metal complexes were prepared by dissolving 0.1000 g of the 4,4'-(((2*E*,5*E*)-hexane-2,5-diylidene)bis(azaneylylidene))bis(1,5-dimethyl-2-phenyl-1,2-dihydro-3*H*-pyrazol-3-one) ligand in a 25 mL round bottom flask in 5 mL of methanol, then adding 0.1829, 0.1808, 0.1829, 0.1862 and 0.1438 g respectively of salt lanthanide $[Ln(NO_3)_3]\cdot 6H_2O$, where Ln = La^{+3}, Nd^{+3}, Er^{+3}, Gd^{+3}, and Dy^{+3} in 5 mL of methanol to prepare the complexes in a molar ratio of 1:1. After reflux stirring the mixture for four to 7 h, the mixture was allowed to precipitate. The precipitate was then collected and cleaned with ether and water to produce a pure precipitate. It is found that all the complexes are soluble in dimethyl sulfoxide and dimethylformamide [24]. Scheme 2 shows the Schiff base ligand's general synthesis of lanthanide complex.

Antibacterial activity

Muller-Hinton (M-H) was prepared by adding 20 mL of the powder into 1.0 L of distilled water and then heating on a burner with shaking. M-H must be autoclaved for 15 min at 121 °C to be sterilized. Then, it

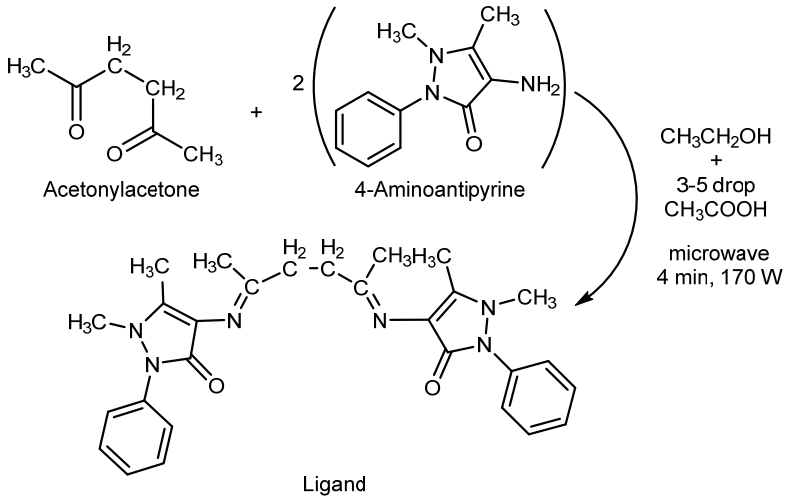

4,4'-(((2*E*,5*E*)-hexane-2,5-diylidene)bis(azaneylylidene))bis(1,5-dimethyl-2-phenyl-1,2-dihydro-3*H*-pyrazol-3-one)

Scheme 1. General synthesis of azomethine Schiff bases

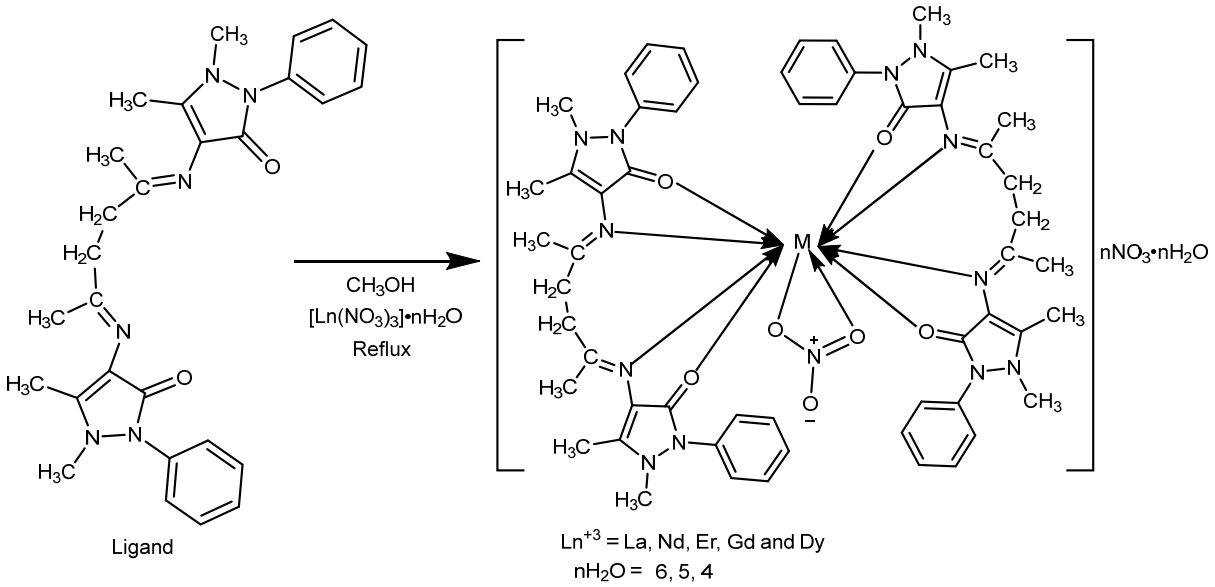

Scheme 2. General synthesis of lanthanide complex

was allowed to cool to 50 °C before pouring into a petri dish. Finally, it was left for about 15 min for solidification before flipping it upside down and storing it in the refrigerator at 4 °C. An agar well diffusion experiment was employed to test the materials' antimicrobial capabilities against Gram-negative and Gram-positive bacteria [25-26]. M-H agar as much as 20 mL was transferred onto sterile Petri plates using an aseptic approach. Several bacterial species were collected from their stock cultures using a sterile wire loop [27]. Once the organisms were cultured, wells with a diameter of 6.0 mm were created on the agar plates using a sterile tip. Various concentrations of the samples were introduced into the bored wells. The cultivated plates, which included samples and the test organisms, were subjected to overnight incubation at 37 °C. Subsequently, the average diameter of the zones of inhibition was measured and recorded [28-29]. Statistical analysis of the data was done using the GraphPad Prism software [30]. The data is presented as the mean ± standard deviation of 3 investigations. A statistically significant difference was observed at a significance level of $p < 0.05$ [31-32].

■ RESULTS AND DISCUSSION

Elemental Analysis

The Schiff bases were prepared using 4-aminoantipyrine and acetonylacetone. The Schiff bases were refined through the process of recrystallization using pure ethanol. Our work resulted in a ligand that can create five new complexes when it reacts with the proper lanthanide nitrate. Various methods can be used to describe the chemical composition of composite materials, which will be discussed in further detail in the following sections. The results of the elemental analysis and physical property measurements of Schiff base and lanthanide complexes are presented in Table 1. These values validate the composition that was initially proposed. The synthesized complexes were formed in a 1:1 (M:L) ratio.

^{1}H-NMR Spectral of Azomethine Ligand

Fig. S1 depicts the ^{1}H-NMR of the Schiff base ligand. The ligand spectra obtained from ^{1}H-NMR analysis display distinct peaks in the ligand, with a solitary peak detected at 2.07 ppm for the N=C–CH_3 group. The –CH_3 alpha molecule exhibits a solitary peak at 2.50 ppm, while the N–N–CH_3 ring of the 4-aminoantipyrine compound displays a single chemical shift at 3.19 ppm. The ^{1}H-NMR spectroscopy technique does not allow for the observation of the chemical shift of the azomethine group C=N due to the absence of a proton associated with the carbon azomethine group. However, it has been observed that the 4-aminoantipyrine ring displays several signals within the range of 7.35–7.55 ppm [22,33].

Table 1. The CHNO analysis and physical characteristics of azomethine ligand L and lanthanide complexes

Compound	Color	M.p. (°C)	Molecular weight (g mol^{-1})	Yield%	Calculated			
					C%	H%	N%	Ln%
Ligand ($C_{28}H_{32}N_6O_2$)	Yellowish white	182	484.60	60%	69.40 (68.95)	6.66 (7.01)	17.34 (17.25)	-
$[La(C_{28}H_{32}N_6O_2)_2{\cdot}NO_3]{\cdot}nNO_3{\cdot}nH_2O$	Light brown	270	1170.12	70%	57.48 (56.56)	5.51 (5.81)	15.56 (15.19)	11.87 (12.42)
$[Nd(C_{28}H_{32}N_6O_2)_2{\cdot}NO_3]{\cdot}nNO_3{\cdot}nH_2O$	White	260	1175.45	70%	57.22 (56.68)	5.49 (6.01)	15.49 (15.34)	12.27 (11.93)
$[Er(C_{28}H_{32}N_6O_2)_2{\cdot}NO_3]{\cdot}nNO_3{\cdot}nH_2O$	Dark brown	270	1198.47	65%	56.12 (55.99)	5.38 (5.29)	15.19 (15.24)	13.96 (14.02)
$[Gd(C_{28}H_{32}N_6O_2)_2{\cdot}NO_3]{\cdot}nNO_3{\cdot}nH_2O$	Dark brown	270	1188.46	65%	56.60 (56.32)	5.43 (5.80)	15.32 (15.11)	13.23 (12.76)
$[Dy(C_{28}H_{32}N_6O_2)_2{\cdot}NO_3]{\cdot}nNO_3{\cdot}nH_2O$	Dark brown	260	1193.71	70%	56.35 (55.95)	5.40 (5.67)	15.25 (15.39)	13.61 (12.96)

^{13}C-NMR Spectrum of Azomethine Ligand

In Fig. S2, the ^{13}C-NMR spectrum of the ligand shows a sharp signal at 162.2 ppm consistent with N=C azomethine carbon. While the resonance signals observed in the region 10.71 ppm CH_3 aliphatic, N=C–CH_3 at 12.63 ppm, C–CH_2 at 36.11 ppm, C–N=C at 106.03 ppm, N–C=C at 153.44 ppm, and C=O at 154.36 ppm. Carbon atoms of aromatic moieties in the ligand were assigned resonance signals in regions 127.23 and 129.13 ppm [34-35].

Mass Spectral of Azomethine Ligand

There is good agreement between the GC-MS spectrum of the $C_{28}H_{32}N_6O_2$ ligand and the proposed molecular structure shown in Scheme 1. The molecular peak confirms ligand identification at 484.60 *m/z*. Fig. S3 illustrates the GC-MS spectrum of the azomethine ligand. The mass spectra of $C_{28}H_{32}N_6O_2$ showed molecular ion peaks at 484.60 g mol^{-1}, which closely matched the calculated values of 484.43 g mol^{-1} [36].

FTIR Spectra of Azomethine Ligand and Its Complexes

A 1% sample was used to record the infrared spectra on the KBR of 4000–400 cm^{-1}. The FTIR spectra of almost the ligand have been meticulously characterized. All these spectra share typical characteristic absorption peaks in the medium range, specifically at 1671, 1619, and 1524 cm^{-1}; these peaks are attributed to C=N, C=O, and C=C bonds, respectively. Upon analysis, the FTIR spectra of 4-aminoantipyrine exhibit two bands of medium intensity, precisely positioned at 3035 and 2915 cm^{-1}. These bands truly capture the mesmerizing and intricate asymmetrical and symmetrical vibrations of the aromatic C–H group [37]. The FTIR spectra of azomethine ligand are illustrated in Fig. S4(a).

As shown in Table 2, the FTIR spectra of the Ln^{+3} complexes changed upon coordination of the Schiff base ligand with the ions La^{+3}, Nd^{+3}, Er^{+3}, $Gd^{+3,}$ and Dy^{+3}. The spectrum revealed the observation of the C=N absorption peak at frequencies of 1650, 1618, 1625, 1624, and 1525 cm^{-1} [38]. In this ensemble, the intensity and location of intricate spectra are altered, indicating that there was coordination. Furthermore, the absorption frequency band at 1687, 1678, and 1678 cm^{-1} can be attributed to the C=O stretching. The stretching of the M–N bond is responsible for the absorption bands observed at the frequencies of 497, 414, 322, 424, and 428 cm^{-1}. An absorption band is observed at frequencies 503, 530, and 505 cm^{-1}, corresponding to M–O stretching band. The broad band at 3458, 3398, 3414, 3421, and 3423 cm^{-1} of all produced complexes can be attributed to O–H of water molecules due to moisture complex formulas but complex spectra [39-40]. The FTIR spectra of azomethine ligand complexed with Ln^{3+} ions are displayed in Fig. S4(b-f).

UV-vis Spectroscopy

The UV-vis spectrum Table 3 recorded in the DMF 1×10^{-3} M solution of all the Ln^{+3} complexes and Schiff base ligand showed maximum absorption bands at 245–385 and 920 cm^{-1} due to the π→π transitions within the aromatic ring n→π and n→π*, respectively. The band observed would be due to n→π* transitions of the C=N and C=O groups of metal-ligand charge transfer coordinate Schiff base lanthanide metal ion, respectively [41]. The metal coordination by the ligand is responsible for this fundamental variant change in each lanthanide

Table 2. The FTIR spectrum revealed in the specific positions of the ligand Schiff bases and Ln^{+3} complexes

Symbol of Ln^{+3} complexes	ν(H–O) cm^{-1} water molecule due to moisture	ν(C–H) cm^{-1} ar.	ν(C–H) cm^{-1} aliph.	ν(C=O) cm^{-1}	ν(C=N) cm^{-1}	ν(C=C) cm^{-1}	ν(NO_3) cm^{-1}	ν(M–O) cm^{-1}	ν(M–N) cm^{-1}
Ligand ($C_{28}H_{32}N_6O_2$)	-	3035	2915	1590	1671	1488	-	-	-
$[La(C_{28}H_{32}N_6O_2)_2{\cdot}NO_3]{\cdot}nNO_3{\cdot}nH_2O$	3458	3037	2926	1687	1650	1525	1496	503	497
$[Nd(C_{28}H_{32}N_6O_2)_2{\cdot}NO_3]{\cdot}nNO_3{\cdot}nH_2O$	3398	3039	2922	1678	1618	1525	1489	530	414
$[Er(C_{28}H_{32}N_6O_2)_2{\cdot}NO_3]{\cdot}nNO_3{\cdot}nH_2O$	3414	3037	2924	1678	1625	1575	1494	505	322
$[Gd(C_{28}H_{32}N_6O_2)_2{\cdot}NO_3]{\cdot}nNO_3{\cdot}nH_2O$	3421	3039	2922	1678	1624	1577	1492	505	424
$[Dy(C_{28}H_{32}N_6O_2)_2{\cdot}NO_3]{\cdot}nNO_3{\cdot}nH_2O$	3423	3041	2922	1678	1525	1577	1494	505	428

Table 3. UV-visible spectra, magnetic susceptibility measurements, and other physical properties of the ligand and its complexes of Ln^{+3} in a solvent DMF and concentration of 1×10^{-3} M

Compound	Configuration Ln^{+3}	No. of unpaired e^-	Conductivity DMF ($cm^2\ ohm^{-1}\ mol^{-1}$)	Absorption bands (nm)	Ground state	Assigned transition	Magnetic susceptibility (B.M)
Ligand ($C_{28}H_{32}N_6O_2$)	-	-	-	245–385; 920	-	π→π, n→π, π→π*	-
$[La(C_{28}H_{32}N_6O_2)_2{\cdot}NO_3]{\cdot}nNO_3{\cdot}nH_2O$	$4f^0$	0	16	-	$^1S_0$	$^1S_0$	Dia
$[Nd(C_{28}H_{32}N_6O_2)_2{\cdot}NO_3]{\cdot}nNO_3{\cdot}nH_2O$	$4f^3$	3	24	582–891; 918–950	$^4I_{9/2}$	$^4I_{9/2}\rightarrow{}^4G_{7/2}$ $^4I_{9/2}\rightarrow{}^2D_{7/2}$ $^4I_{9/2}\rightarrow{}^2P_{1/2}$	4.59
$[Er(C_{28}H_{32}N_6O_2)_2{\cdot}NO_3]{\cdot}nNO_3{\cdot}nH_2O$	$4f^{11}$	3	30	487–521; 541–652; 803	$^4I_{15/2}$	$^4I_{15/2}\rightarrow{}^4I_{15/2}$ $^4I_{15/2}\rightarrow{}^4G_{11/2}$	2.09
$[Gd(C_{28}H_{32}N_6O_2)_2{\cdot}NO_3]{\cdot}nNO_3{\cdot}nH_2O$	$4f^7$	7	25	758–808; 914	$^8S_{7/2}$	$^8S_{7/2}\rightarrow{}^6I_{7/2}$	2.97
$[Dy(C_{28}H_{32}N_6O_2)_2{\cdot}NO_3]{\cdot}nNO_3{\cdot}nH_2O$	$4f^9$	5	27	621–636; 814–920	$^6H_{15/2}$	$^6H_{5/2}\rightarrow{}^5I_{11}$ $^6H_{15/2}\rightarrow{}^6P_{5/2}$	4.02

complex involving La, Nd, Er, Gd, and Dy. Upon completion, the higher energy band in the free ligand is observed as a single band with little frequency shift. Due to the well-protected $5s^2$ and $5p^6$ orbitals, a plausible schematic representation of the lanthanide complex ions indicates that direct bonding is impossible, as determined by analytical and spectral data. Therefore, ligands mainly do not alter the properties of Ln^{+3} ions [42]. Lanthanides complex exhibit a significantly more distinct electronic spectrum when compared to *d*-block metals. Lanthanide absorption spectra are typically obtained via *4f–4f* transitions, which are similar to transition metal *d-d* transitions. In contrast to transition metals, lanthanide elements often exhibit distinct, linear absorption spectra. The lanthanides are located deep within an atom, which allows them to reduce the extensive impact of ligand vibrations [43-44]. Fig. S5 shows UV-vis spectra of the Schiff base ligand and some of its complexes with Ln^{3+} ions. The electronic spectrum of the Ln^{+3} complexes and the synthesized compounds is displayed.

Magnetic Sensitivity Measurement

Single-electron magnetic sensitivity studies are one of the basic and successful procedures that complement other diagnostic procedures to propose spatial forms of complexes. The compound is paramagnetic if the center atom possesses one or more electrons. Since all lanthanide elements' electronic distributions except *for* f^0 and f^{14} contain only single electrons, they are classified as paramagnetic [45]. The difference between these lanthanide elements and transitional elements is that their magnetic moment does not agree with the spin equation moment [46], meaning that the value of this to spin magnetic moment cannot be calculated using the Eq. (1);

$$\mu_{eff} = \sqrt{4(S+1)+l(L+1)} \quad (1)$$

The following Table 3 contains the properties of the elements of type *4f*. The progressive filling of the *4f* orbitals occurs after the substantial penetration of the *f* orbitals, which are effectively shielded by the filled *5s*, *5p*, and *6s* sub-shells (for atoms) at atomic number 57. Consequently, the extent of interaction with ligand orbitals is negligible, the bonding within lanthanide complexes is merely weakly covalent, the ligands' steric properties dictate the stereochemistry of the complexes, and ligand-field effects are negligible. Thus, the metal ion's environment has little impact on its spectroscopic and magnetic properties [47]. Table 3 details the characteristics of lanthanides and their trivalent ions.

Molar Conductivity Measurements

Table 3 presents the recorded molar conductivity of Ln^{+3} complexes in DMF solutions at 25 °C [48]. The internal coordination domain of all complexes contains nitrate ions. The molar conductance values of the complexes in DMF solvent range from 16 to 30 $cm^2\ ohm^{-1}\ mol^{-1}$, indicating that the complexes are non-electrolytic. This is supported by the magnetic values

Table 4. The effect of the azomethine ligand $C_{28}H_{32}N_6O_2$ and its Ln^{+3} complexes dissolved in DMSO at the concentration 1×10^{-3} M on 4 types of bacteria

Compounds	*E. coli*	*S. aureus*	*K. pneumoniae*	*S. mutans*
Ligand ($C_{28}H_{32}N_6O_2$)	6	12	7	13
$[La(C_{28}H_{32}N_6O_2)_2{\cdot}NO_3]{\cdot}nNO_3{\cdot}nH_2O$	6	14	7	16
$[Nd(C_{28}H_{32}N_6O_2)_2{\cdot}NO_3]{\cdot}nNO_3{\cdot}nH_2O$	6	17	10	18
$[Er(C_{28}H_{32}N_6O_2)_2{\cdot}NO_3]{\cdot}nNO_3{\cdot}nH_2O$	6	16	7	15
$[Gd(C_{28}H_{32}N_6O_2)_2{\cdot}NO_3]{\cdot}nNO_3{\cdot}nH_2O$	6	17	9	17
$[Dy(C_{28}H_{32}N_6O_2)_2{\cdot}NO_3]{\cdot}nNO_3{\cdot}nH_2O$	6	24	12	22

falling within the reported range for electrolytes with a 1:1 ratio [49-50].

Antibacterial Action

Various strains of *E. coli*, *S. aureus*, *K. pneumoniae*, and *S. mutans* were tested for their antibacterial activity against ligand and their lanthanide metal chelate. The compounds were evaluated using the paper disc diffusion method, at a volume of 1 μL in a DMSO solution. The diameter of the susceptibility zones was measured, and the results are presented in Table 4. The measurement of susceptibility zones was conducted in the vicinity of the bactericidal disks. The inhibitory effects on the growth of the examined bacterial species varied among the Schiff bases and their complexes when evaluated individually. The findings of the study indicate that the antibacterial efficacy of the ligand Schiff base compounds was enhanced when they were coordinated with the lanthanide ions La, Nd, Er, Gd, and Dy. The antibacterial impact of lanthanide ions on bacterial species exhibits variability [51]. The Dy^{+3} complex exhibited more excellent antibacterial activity against one species and comparatively lower antibacterial activity against the other species than the La^{+3} complex. Similar findings were observed for several metal complexes. However, it is not feasible to determine the specific metal ion that has a greater antibacterial effect on one bacterial species compared to another. However, it is conclusive that metal ions do indeed play a substantial part in augmenting the antibacterial efficacy of chelation agents. In the chelated complex, the metal ion's positive charge is proposed to be partially distributed across the donor atoms, resulting in π electron delocalization throughout the entire chelate ring. This phenomenon enhances the lipophilic nature of the metal chelate, promoting its ability to permeate the lipoid layers in the bacterial membranes. The presence of metal ions is believed to alter parameters such as solubility, dipole moment, and cell permeability mechanisms, hence boosting the bactericidal properties of metals. We are currently doing *in vitro* experiments to investigate the specific mechanism responsible for this action [52-55].

This study used *E. coli*, *S. aureus*, *K. pneumoniae*, and *S. mutans* as bacterial strains to determine their antibacterial properties. According to the results, metal complexes exhibited greater antibacterial activity than synthesized Schiff bases L. The *E. coli* was less active than the standard *S. aureus*, *K. pneumoniae*, and *S. mutans*. The *S. mutans* and *S. aureus* showed the highest action towards Schiff bases ligand and lanthanide complexes, with a maximum activity of 24 nm. Table 4 and Fig. S6 show the result of antibacterial activity for all compounds.

■ CONCLUSION

The azomethine ligand (Schiff base) was synthesized and characterized by analytical and spectral techniques, and then a series containing five lanthanide metal complexes was also conducted. The molar conductance value of metal complexes indicates their non-electrolytic nature at 25 °C, and the stability of the lanthanide complexes was demonstrated. The spectroscopic results unequivocally demonstrate that the complexes possess a specific makeup. From the analysis of spectroscopic data, it may be inferred that the center metal ion. The complexes are coordinated to a total of 6 oxygen atoms, with 2 coming from the nitrate and 4 from the antipyrine ligand. Additionally, there are 4 nitrogen atoms involved. These complexes are generated

via the bonding between the C=N and C=O. The formula for all mineral complexes is $[Ln^{+3}(L)_2(NO_3)]\cdot nH_2O$. The form of complexes La, Nd, Er, Gd, and Dy was built based on spectra, analytical data, and attributed geometries. These compounds exhibited significant activity against all the tested microorganisms.

ACKNOWLEDGMENTS

We would like to thank all those who provided assistance and advice, along with the research supervisor who led the research and those who cooperated with us and provided a conducive environment for the study. The magazine editors and auditors who contributed to the research process are also appreciated.

CONFLICT OF INTEREST

The authors state that a conflict of interest does not exist.

AUTHOR CONTRIBUTIONS

Kawther Adeeb Hussein developed this idea based on the expressions of Naser Shaalan and Mawar Faeq. Kawther Adeeb Hussein and Mawar Faeq carried out the experiment, wrote the manuscript, and performed the analysis. Naseer Shaalan supervised the project. The results were discussed, and all authors wrote the final manuscript.

REFERENCES

[1] Singh, C., Khanna, V., and Singh, S., 2023, Sustainability of microwave heating in materials processing technologies, *Mater. Today: Proc.*, 73, 241–248.

[2] Margetic, D., 2024, Mechanochemical and microwave multistep organic reactions, *Curr. Green Chem.*, 11 (2), 172–193.

[3] Zhang, Y., 2017, The Application of Microwave Technology in Chemistry and Chemical Engineering, *Proceedings of the 2016 International Conference on Engineering Management*, Atlantis Press, Dordrecht, Netherlands, 50–53.

[4] Taha, Z.A., Hijazi, A.K., and Al Momani, W.M., 2020, Lanthanide complexes of the tridentate Schiff base ligand salicylaldehyde-2-picolinoylhydrazone: Synthesis, characterization, photophysical properties, biological activities and catalytic oxidation of aniline, *J. Mol. Struct.*, 1220, 128712.

[5] Soliman, A.I.A., Sayed, M., Elshanawany, M.M., Younis, O., Ahmed, M., Kamal El-Dean, A.M., Abdel-Wahab, A.M.A., Wachtveitl, J., Braun, M., Fatehi, P., and Tolba, M.S., 2022, Base-free synthesis and photophysical properties of new Schiff bases containing indole moiety, *ACS Omega*, 7 (12), 10178–10186.

[6] Boulechfar, C., Ferkous, H., Delimi, A., Djedouani, A., Kahlouche, A., Boublia, A., Darwish, A.S., Lemaoui, T., Verma, R., and Benguerba, Y., 2023, Schiff bases and their metal complexes: A review on the history, synthesis, and applications, *Inorg. Chem. Commun.*, 150, 110451.

[7] Hussain, E.M., 2023, Synthesis and antibacterial evaluation for some new Schiff-bases derived from *p*-amino acetanilide, *Baghdad Sci. J.*, 20 (6), 2455–2455.

[8] Kargar, H., Fallah-Mehrjardi, M., and Munawar, K.S., 2024, Metal complexes incorporating tridentate ONO pyridyl hydrazone Schiff base ligands: Crystal structure, characterization and applications, *Coord. Chem. Rev.*, 501, 215587.

[9] Abd AL_Qadir, N.A., and Shaalan, N.D., 2023, Synthesis, characterization and biological activity study for some new metals complexes with (3*Z*,3'*E*)-3,3'-(((2*E*,5*E*)-hexane-2,5-diylidene)bis(hydrazine-2,1-diylidene))bis(indolin-2-one), *Ibn AL-Haitham J. Pure Appl. Sci.*, 36 (3), 231–244.

[10] Yimer, A.M., 2015, Review on preparation and description of some first series divalent transition metal complexes with novel Schiff's base ligands, *Rev. Catal.*, 2 (1), 14–25.

[11] Kumar, R., Singh, A.A., Kumar, U., Jain, P., Sharma, A.K., Kant, C., and Haque Faizi, M.S., 2023, Recent advances in synthesis of heterocyclic Schiff base transition metal complexes and their antimicrobial activities especially antibacterial and antifungal, *J. Mol. Struct.*, 1294, 136346.

[12] Al-Adilee, K.J., Jawad, S.H., Kyhoiesh, H.A.K., and Hassan, H.M., 2024, Synthesis, characterization, biological applications, and molecular docking

studies of some transition metal complexes with azo dye ligand derived from 5-methyl imidazole, *J. Mol. Struct.*, 1295, 136695.

[13] Gomaa, A.I., Gomaa, E.A., Zaky, R.R., and Abd El-Hady, M.N., 2024, Design and synthesis of pyridine bis-hydrazone metal complexes of Co(II), Cu(II), and Hg(II): Spectral, Gaussian, electrochemical, biological, drug-likeness and molecular docking investigations, *Inorg. Chem. Commun.*, 162, 112188.

[14] Mohan, B., and Shaalan, N., 2023, Synthesis, spectroscopic, and biological activity study for new complexes of some metal ions with Schiff bases derived from 2-hydroxy naphthaldehyde with 2-amine benzhydrazide, *Ibn Al-Haitham J. Pure Appl. Sci.*, 36 (1), 208–224.

[15] Janjua, U.U., Pervaiz, M., Ali, F., Saleem, A., Ashraf, A., Younas, U., and Iqbal, M., 2023, Schiff base derived Mn(II) and Cd(II) novel complexes for catalytic and antioxidant applications, *Inorg. Chem. Commun.*, 157, 111233.

[16] Kumar, M., Singh, A.K., Singh, V.K., Yadav, R.K., Singh, A.P., and Singh, S., 2024, Recent developments in the biological activities of 3d-metal complexes with salicylaldehyde-based N, O-donor Schiff base ligands, *Coord. Chem. Rev.*, 505, 215663.

[17] Sakthivel, A., Jeyasubramanian, K., Thangagiri, B., and Raja, J.D., 2020, Recent advances in Schiff base metal complexes derived from 4-aminoantipyrine derivatives and their potential applications, *J. Mol. Struct.*, 1222, 128885.

[18] Youns, N.M., 2024, Synthesis, characterization and antimicrobial activity of new 4-aminoantipyrine derivatives using ultrasonic mediation, *Baghdad Sci. J.*, Online-First (9).

[19] Lal Singh, H., Kulhari, P., Choudhary, G., and Khaturia, S., 2024, Synthesis, spectral, DFT, and antibacterial studies of nickel(II) and cobalt(II) complexes with aminoantipyrine based Schiff base ligands, *Inorg. Chem. Commun.*, 162, 112192.

[20] Narayanswamy, A., Ramakrishna, D., Shekar, P.V.R., Rajendrachari, S., and Sudhakar, R., 2024, Quantum chemical and experimental evaluation of a 4-amino-antipyrine based Schiff base as corrosion inhibitor for steel material, *ACS Omega*, 9 (11), 13262–13273.

[21] Ebosie, N.P., Ogwuegbu, M.O.C., Onyedika, G.O., and Onwumere, F.C., 2021, Biological and analytical applications of Schiff base metal complexes derived from salicylidene-4-aminoantipyrine and its derivatives: A review, *J. Iran. Chem. Soc.*, 18 (12), 3145–3175.

[22] Hussein, K.A., and Shaalan, N., 2021, Synthesis, spectroscopy and biological activities studies for new complexes of some lanthanide metals with Schiff's bases derived from dimedone with 4-aminoantipyrine, *Chem. Methodol.*, 6 (2), 103–113.

[23] Shaalan, N., 2022, Preparation, spectroscopy, biological activities and thermodynamic studies of new complexes of some metal ions with 2-[5-(2-hydroxy-phenyl)-1,3,4-thiadiazol-2-ylimino]-methyl-naphthalen-1-ol, *Baghdad Sci. J.*, 19 (4), 0829–0829.

[24] Hussein, K.A., and Shaalan, N., 2022, Synthesis, characterization, and antibacterial activity of lanthanide metal complexes with Schiff base ligand produced from reaction of 4,4-methylene diantipyrine with ethylenediamine, *Indones. J. Chem.*, 22 (5), 1365–1375.

[25] Bahjat, H.H., Ismail, R.A., Sulaiman, G.M., and Jabir, M.S., 2021, Magnetic field-assisted laser ablation of titanium dioxide nanoparticles in water for anti-bacterial applications, *J. Inorg. Organomet. Polym. Mater.*, 31 (9), 3649–3656.

[26] Khashan, K.S., Abdulameer, F.A., Jabir, M.S., Hadi, A.A., and Sulaiman, G.M., 2020, Anticancer activity and toxicity of carbon nanoparticles produced by pulsed laser ablation of graphite in water, *Adv. Nat. Sci: Nanosci. Nanotechnol.*, 11 (3), 035010.

[27] Khashan, K.S., Badr, B.A., Sulaiman, G.M., Jabir, M.S., and Hussain, S.A., 2021, Antibacterial activity of zinc oxide nanostructured materials synthesis by laser ablation method, *J. Phys.: Conf. Ser.*, 1795 (1), 012040.

[28] Jihad, M.A., Noori, F.T.M., Jabir, M.S., Albukhaty, S., AlMalki, F.A., and Alyamani, A.A., 2021,

Polyethylene glycol functionalized graphene oxide nanoparticles loaded with *Nigella sativa* extract: A smart antibacterial therapeutic drug delivery system, *Molecules*, 26 (11), 3067.

[29] Mohammed, M.K.A., Mohammad, M.R., Jabir, M.S., and Ahmed, D.S., 2020, Functionalization, characterization, and antibacterial activity of single wall and multi wall carbon nanotubes, *IOP Conf. Ser.: Mater. Sci. Eng.*, 757 (1), 012028.

[30] Ali, I.H., Jabir, M.S., Al-Shmgani, H.S.A., Sulaiman, G.M., and Sadoon, A.H., 2018, Pathological and immunological study on infection with *Escherichia coli* in ale BALB/c mice, *J. Phys.: Conf. Ser.*, 1003 (1), 012009.

[31] Younus, A., Al-Ahmer, S., and Jabir, M., 2019, Evaluation of some immunological markers in children with bacterial meningitis caused by *Streptococcus pneumoniae*, *Res. J. Biotechnol.*, 14, 131–133.

[32] Jabir, M.S., Rashid, T.M., Nayef, U.M., Albukhaty, S., AlMalki, F.A., Albaqami, J., AlYamani, A.A., Taqi, Z.J., and Sulaiman, G.M., 2022, Inhibition of *Staphylococcus aureus* α-hemolysin production using nanocurcumin capped Au@ZnO nanocomposite, *Bioinorg. Chem. Appl.*, 2022 (1), 2663812.

[33] Wang, Y.F., 2021, Borinic Acid-Catalyzed Ring-Opening of Epoxy Alcohols, *Dissertation*, University of Toronto, Canada.

[34] Khalil, M.H., and Abdullah, F.O., 2024, Synthesis, characterization, and anticancer and antioxidant activities of novel complexes of palladium and an organic Schiff-base ligand, *Bull. Chem. Soc. Ethiop.*, 38 (3), 605–613.

[35] Gavali, L.V., Mohammed, A.A., Al-Ogaili, M.J., Gaikwad, S.H., Kulkarni, M., Das, R., and Ubale, P.A., 2024, Novel terephthalaldehyde bis (thiosemicarbazone) Schiff base ligand and its transition metal complexes as antibacterial agents: Synthesis, characterization and biological investigations, *Results Chem.*, 7, 101316.

[36] Shaalan, N., Fadel, Z.H., Mahmood, W.A., and Al-Hamdani, A.A.S., 2016, Synthesis and characterization studies of metal complexes with Schiff base derived from 4-[5-(2-hydoxy-phenyl)-[1,3,4-oxadiazol-2-ylimino methyl]-1,5-dimethyl-2-phenyl-1,2-dihydro-pyrazol-3-one, *Baghdad Sci. J.*, 13 (2), 19–28.

[37] Hussein, K.A., Shaalan, N., Lafta, A.K., and Al Akeedi, J.M., 2024, Preparation, characterization, and biological activity of La(III), Nd(III), Er(III), Gd(III), and Dy(III) complexes with Schiff base resulted from reaction of 4-antipyrinecarboxaldehyde and 2-aminobenzothiazole, *Indones. J. Chem.*, 24 (2), 358–369.

[38] Abdulrazzaq, A.G., and Al-Hamdani, A.A.S., 2023, Ni^{2+}, Pt^{4+}, Pd^{2+}, and Mn^{2+} metal ions complexes with azo derived from quinolin-2-ol and 3-amino-*N*-(5-methylisoxazol-3-yl) benzenesulfonamide: Synthesis, characterization, thermal study, and antioxidant activity, *Baghdad Sci. J.*, 20 (6), 2207–2223.

[39] Hussein, K.A., Mahdi, S., and Shaalan, N., 2023, Synthesis, spectroscopy of new lanthanide complexes with Schiff base derived from (4-antipyrinecarboxaldehyde with ethylene di-amine) and study the bioactivity, *Baghdad Sci. J.*, 20 (2), 469–482.

[40] Cruz-Navarro, A., Rivera, J.M., Durán-Hernández, J., Castillo-Blum, S., Flores-Parra, A., Sánchez, M., Hernández-Ahuactzi, I., and Colorado-Peralta, R., 2018, Luminescence properties and DFT calculations of lanthanide (III) complexes (Ln = La, Nd, Sm, Eu, Gd, Tb, Dy) with 2,6-bis (5-methyl-benzimidazol-2-yl)pyridine, *J. Mol. Struct.*, 1164, 209–216.

[41] Li, M., Dong, H., Chen, Y., Hao, W., Wang, Y., Zhang, Y., Zhang, Z., Hao, Y., Zhou, Y., Li, F., and Liu, L., 2024, A dual-ligand lanthanide-based metal–organic framework for highly selective and sensitive colorimetric detection of Fe^{2+}, *Anal. Methods*, 16 (6), 899–906.

[42] Evsiunina, M.V., Khult, E.K., Matveev, P.I., Kalle, P., Lemport, P.S., Petrov, V.S., Aksenova, S.A., Nelyubina, Y.V., Koshelev, D.S., Utochnikova, V.V., Petrov, V.G., Ustynyuk, Y.A., and Nenajdenko, V.G., 2024, Unravelling the

mechanism of *f*-element extraction by phenanthroline-diamides: A case of 4,7-substituted 1,10-phenanthroline-2,9-diamides, *Sep. Purif. Technol.*, 339, 126621.

[43] Sivakumar, R., and Lee, N.Y., 2024, Recent advances in luminescent lanthanides and transition metal complex-based probes for imaging reactive oxygen, nitrogen, and sulfur species in living cells, *Coord. Chem. Rev.*, 501, 215563.

[44] Schwarz, N., Krätschmer, F., Suryadevara, N., Schlittenhardt, S., Ruben, M., and Roesky, P.W., 2024, Synthesis, structural characterization, and magnetic properties of lanthanide arsolyl sandwich complexes, *Inorg. Chem.*, 63 (21), 9520–9526.

[45] Abdulrazzaq, A.G., and Al-Hamdani, A.A.S., 2024, Synthesis, characterization, thermal analysis study and antioxidant activity for some metal ions Cr(III), Fe(III), Mn(II) and Pd(II) complexes with azo dye derived from *p*-methyl-2-hydroxybenzaldehyde, *Baghdad Sci. J.*, 21 (6), 1960–1982.

[46] Gil, Y., and Aravena, D., 2024, Understanding single-molecule magnet properties of lanthanide complexes from 4f orbital splitting, *Dalton Trans.*, 53 (5), 2207–2217.

[47] Kim, T., Jeon, H., Lee, J.R., and Kim, D., 2024, Magnetic separation-enhanced photoluminescence detection of dipicolinic acid and quenching detection of Cu(II) ions, *Spectrochim. Acta, Part A*, 305, 123501.

[48] Al-Hamdani, A.A.S., Shaalan, N., Hassan, S.S., and Hasan, Z.A.A.H., 2016, Preparation and spectroscopic studies of some metal ion complexes of 2-((4-formyl-3-hydroxynaphthalen-2-yl)diazenyl)benzoic acid, *Baghdad Sci. J.*, 13 (2), 95–104.

[49] Nassar, H., Abou-El-Wafa, M.H.M., and Elkik, H., 2024, Synthesis and characterization of some coordinated metal and charge transfer complexes of isonicotinic acid hydrazide ligand with 2-hydroxyacetophenonylidene, *Spectrochim. Acta, Part A*, 309, 123759.

[50] Arnaouti, E., Georgiadou, C., Hatizdimitriou, A.G., Kalogiannis, S., and Psomas, G., 2024, Erbium(III) complexes with fluoroquinolones: Structure and biological properties, *J. Inorg. Biochem.*, 255, 112525.

[51] Iacopetta, D., Ceramella, J., Catalano, A., Mariconda, A., Giuzio, F., Saturnino, C., Longo, P., and Sinicropi, M.S., 2023, Metal complexes with Schiff bases as antimicrobials and catalysts, *Inorganics*, 11 (8), 320.

[52] Bayeh, Y., Mohammed, F., Gebrezgiabher, M., Elemo, F., Getachew, M., and Thomas, M., 2020, Synthesis, characterization, and antibacterial activities of polydentate Schiff bases, based on salicylaldehyde, *Adv. Biol. Chem.*, 10 (5), 127–139.

[53] Abd El-Halim, H., El-Sayed, O.Y., and Mohamed, G.G., 2023, Anti-carcinoma and anti-microbial behavioral studies for octahedral synthesized Schiff base metal complexes, *J. Iran. Chem. Soc.*, 20 (11), 2713–2725.

[54] Al-Hajjar, R.L.N., Taha, E.M., Farhan, A.M., and Shaalan, N., 2023, Enzymatic assay of immobilized β-D-galactosidase enzyme on magnetite nanoparticle, *Iraqi J. Sci.*, 64 (2), 6093–6103.

[55] Reda, S.M., and Al-Hamdani, A.A.S., 2023, Mn(II), Fe(III), Co(II) and Rh(III) complexes with azo ligand: Synthesis, characterization, thermal analysis, and bioactivity, *Baghdad Sci. J.*, 20 (3), 642–660.